

X-RAY OBSERVATIONS OF THE COMPACT CENTRAL OBJECT IN SUPERNOVA REMNANT
G347.3–0.5J. S. LAZENDIC¹, P. O. SLANE¹, B. M. GAENSLER¹, P. P. PLUCINSKY¹,
J. P. HUGHES², D. K. GALLOWAY³ AND F. CRAWFORD⁴*Draft version October 30, 2018*

ABSTRACT

We present *Chandra*, *XMM-Newton* and *RXTE* observations of 1WGA J1713.4–3949, a compact source at the center of the galactic supernova remnant (SNR) G347.3–0.5. The X-ray spectrum of the source is well-fitted by the sum of a blackbody component with a temperature of ~ 0.4 keV plus a power law component with photon index ~ 4 . We found no pulsations down to 4% in the 0.01–0.16 Hz range and down to 25% in the 0.01–128 Hz range. This source resembles other compact central objects (CCOs) in SNRs, and we suggest that 1WGA J1713.4–3949 is the associated neutron star for G347.3–0.5. We also measured the properties of the adjacent radio pulsar PSR J1713–3945 with a 392 ms period and show that it is not associated with 1WGA J1713.4–3949 nor, most probably, with SNR G347.3–0.5 as well.

Subject headings: ISM: individual (G347.3–0.5) — pulsars: individual (J1713–3945) — stars: neutron (1WGA J1713.4–3949) — supernova remnants — X-rays: stars

1. INTRODUCTION

For many years it has been well known that pulsars — compact remains of supernova explosions — are rapidly rotating, highly magnetized neutron stars (NSs). However, sources discovered in recent years have shown that NSs also appear to come in other varieties: even more highly magnetized objects with slow spins, such as anomalous X-ray pulsars (AXPs) and soft gamma-ray repeaters (SGRs) (e.g., Mereghetti 1998; Thompson 2000), and more poorly understood objects near the centers of SNRs with detectable X-ray flux, but no optical/radio counterparts or signs of rotation, so-called compact central objects (CCOs; Pavlov et al. 2002). Their spectra are very soft, with blackbody temperatures ~ 0.4 keV, often requiring additional power law component with photon indices of ~ 4 (Pavlov et al. 2002). In this article we address the nature of 1WGA J1713.4–3949, a compact source located at the center of the SNR G347.3–0.5 (RX J1713.7–3946). Early *ROSAT* observations identified two point sources within the boundaries of the SNR shell (Pfeffermann & Aschenbach 1996, ; see also Figure 1). The source further away from the center of the remnant, 1WGA J1714.4–3945, was determined to be of stellar origin (Pfeffermann & Aschenbach 1996). For the other source, 1WGA J1713.4–3949, located at the geometrical center of the SNR, no optical counterpart has been found within $10''$ of the *ROSAT* position (Slane et al. 1999), and the source has correspondingly been suggested to be a candidate for an associated neutron star. While *ASCA* observations were not able to provide useful limits to the pulsations in the X-ray band (Slane et al. 1999), radio pulsations were detected with a 392 ms period within a $7'$ radius region towards this source (PSR J1713–3945 Crawford et al. 2002).

1WGA J1713.4–3949 has been observed with the *Chandra X-ray Observatory* as a part of a project to study nonthermal radio and X-ray emission from the SNR shell

(Lazendic et al. 2003). In this paper we present a detailed spectral and timing analysis of 1WGA J1713.4–3949 using our *Chandra* data, as well as archival data from the *XMM-Newton* and *RXTE* satellites. We also present properties of the radio pulsar PSR J1713–3945, which imply it is not related to 1WGA J1713.4–3949 or SNR G347.3–0.5.

2. OBSERVATIONS

Two fields towards G347.3–0.5 were observed on 2000 July 25 with the Advanced CCD Imaging Spectrometer (ACIS) detector on board the *Chandra X-ray Observatory* (ObsID 736 and 737). The ACIS-I detector for ObsID 736 was positioned at the bright northwestern rim of the SNR and the roll angle was such that 1WGA J1713.4–3949 fell on the S1 chip (see Figure 1). Data were taken in timed exposure mode with an integration time of 3.2 s per frame. The fully processed Level 2 data were reduced using standard threads in the CIAO software package version 2.2.1. The effective exposure time after data processing was 29.6 ks. The exposure-corrected *Chandra* image of the SNR and the compact source 1WGA J1713.4–3949 is shown in Figure 1, with the *ROSAT* contours overlaid. The image was binned in $4''6 \times 4''6$ pixels and smoothed with a Gaussian filter with a FWHM of $2''$. The image of the compact source is elongated because its location is well off-axis ($\sim 23'$) from the aim point.

We obtained archival *XMM* data of 1WGA J1713.4–3949 carried out on 2001 March 2 with a 15 ks exposure (ObsID 0093670501; see also Cassam-Chenai et al. 2003). The European Photon Imaging Camera (EPIC)-pn camera was operated in Extended Full Frame mode with time resolution of 199 ms, while the two EPIC-MOS cameras were operated in Full Frame mode with a time resolution of 2.6 s. The EPIC data reduction was performed using the SAS software package version 5.4.1. The event files used for analysis were created from observational data files

¹ Harvard-Smithsonian Center for Astrophysics, 60 Garden Street, Cambridge, MA 02138, jlazendic@cfa.harvard.edu

² Department of Physics and Astronomy, Rutgers University, 136 Frelinghuysen Road, Piscataway, NJ 08854

³ Center for Space Research, Massachusetts Institute of Technology, Cambridge, MA 02139

⁴ Department of Physics, Haverford College, Haverford, PA 19041

(ODFs) using the SAS tasks `epchain` and `emchain`. The net exposure time after filtering event files for good time intervals was 9.2 ks in the pn camera and 14.1 ks in each MOS camera.

We used archival data of SNR G347.3–0.5 (Pannuti et al. 2003) from the Proportional Counter Array (PCA) aboard the *RXTE* satellite, which is sensitive to X-ray photons in the energy band 2–60 keV and has a field of view with radius $\approx 1^\circ$. While the PCA has no imaging capability, it has a large effective area (6000 cm²) which makes it suitable for searching for faint X-ray pulsations. Observations of G347.3–0.5 were made in 7 separate intervals between 1999 June 14–24, with a total exposure time of 100 ks. Analysis of the *RXTE* data was carried out using LHEASOFT software version 5.2.

A 392-ms radio pulsar, PSR J1713–3945, was discovered in a 20 cm targeted search for pulsations in SNR G347.3–0.5 using the Parkes telescope and multibeam receiver. The details of the search and discovery are outlined in Crawford et al. (2002). The pulsar was subsequently timed with the multibeam receiver at Parkes to obtain astrometric and spin parameters and to determine whether the pulsar was associated with 1WGA J1713.4–3949.

3. ANALYSIS AND RESULTS

3.1. Spectral Analysis

For the spectral analysis of the *Chandra* data, we extracted the source counts from a $37'' \times 61''$ elliptical region around the compact source, and for the background region we used a $2' \times 3'$ elliptical region north of the source. We obtained 8454 ± 103 background-subtracted counts for the source and the spectrum was grouped to contain at least 25 counts per bin. Residuals from fitting standard continuum models to the source spectrum (blackbody, bremsstrahlung and power law) revealed an apparent change in the gain calibration on chip S1 that results in a spurious absorption feature around 2 keV. We extracted data from the on-board calibration source taken before and after our observation, and these show that there is indeed a gain shift for this CCD of $\sim 3.5\%$. However, we found that the fit parameters did not change significantly when the gain was frozen at this 3.5% value or when it was left as a free parameter. We thus allowed gain to vary in our models (see Table 1).

For spectral analysis of the *XMM* data, we obtained 9600 ± 217 background-subtracted counts from the pn camera, and 5451 ± 74 (5274 ± 73) in the MOS1 (MOS2) camera. In the pn camera, the counts were extracted from a $27''$ radius circular region around the source, and for the background extraction we used a $3/4 \times 8/3$ box north from the source position inside the same CCD chip. Similarly, in the MOS1 (MOS2) camera we used $22''$ ($19''$) radius circular region for the source and $3/4$ ($2/2$) radius circular region on the same chip for the background. The spectra were also grouped to contain at least 25 counts per bin. We performed a joint spectral analysis of the three EPIC data sets, allowing only the relative normalization to vary. The results obtained were consistent with those obtained from the *Chandra* spectrum. We therefore proceeded with a joint spectral analysis of *Chandra* and *XMM* spectra.

The results from fitting a few typical neutron star mod-

els are summarized in Table 1 and a fit example is given in Figure 2. Fits with the bremsstrahlung and blackbody models gave equally acceptable results, while the power law model gave a somewhat higher reduced χ^2 . The steep photon index of $\Gamma \sim 4$ excludes the possibility that 1WGA J1713.4–3949 is a background active galactic nucleus (AGN), which typically have photon indices of 1.2–2.2 (Turner & Pounds 1986). The best-fit column density (N_H) in the power law model of $\sim 11 \times 10^{21} \text{ cm}^{-2}$ is also somewhat higher than the value of $8 \times 10^{21} \text{ cm}^{-2}$ found towards the SNR (Lazendic et al. 2003). On the other hand, a blackbody model yields $N_H \sim 4 \times 10^{21} \text{ cm}^{-2}$, which is a lower value than found towards the SNR. The blackbody fit is improved by adding a power law component, which also results in an N_H value consistent with that found towards the SNR. In this composite spectrum the unabsorbed source luminosity is $L_X(0.5 - 10.0 \text{ keV}) \sim 6 \times 10^{34} \text{ erg s}^{-1}$, adopting a distance of $\sim 6 \text{ kpc}$ to the SNR (Slane et al. 1999). The blackbody normalization yields a relatively small emitting area with radius $R \sim 2.4 D_{6\text{kpc}} \text{ km}$, which is significantly smaller than the canonical value for the NS radius of 10 km. This could imply that most of the thermal emission originates from the polar caps on the NS surface, while the thermal component from the rest of the NS surface is too faint to be detected.

The small inferred radius may be due, at least partly, to oversimplification of the thermal emission from the NS by the blackbody model. More appropriate models that take into account the NS atmosphere (NSA) yield lower NS temperatures, which in turn correspond to larger NS radii (e.g., Zavlin, Pavlov, & Shibano 1996). To investigate this, we fit our spectra with two NSA models. The NSA model by Gansicke, Braje, & Romani (2002) is calculated for weakly magnetic NS ($B \leq 10^{10} \text{ G}$) and considers hydrogen, solar or iron compositions of the atmosphere. The NSA model by Pavlov et al. (1995) assumes the standard magnetic field strength ($B = 10^{12} \text{ G}$) and hydrogen atmosphere. Both models assume a standard NS mass of $1.4 M_\odot$. Both hydrogen models gave acceptable residuals and yielded emitting region sizes close to 10 km, with corresponding reductions in the NS temperature. For either model, however, the derived temperature is above the expected surface temperature for a cooling neutron star more than several hundred years old. Model atmospheres with solar abundance or iron composition gave unacceptable fits predicting broad absorption features not present in the spectra.

3.2. Timing Analysis

We used a Fast-Fourier Transform (FFT) to search the X-ray data for pulsations from 1WGA J1713.4–3949, but found no pulsed signal; we list upper limits on the pulsed fraction and the search parameters in Table 2. The upper limit from *RXTE* data is least constraining because 1WGA J1713.4–3949 only accounts for 0.6% of the total flux in the *RXTE*'s large field of view.

To derive the timing properties of the radio pulsar PSR J1713–3945 the TEMPO timing package⁵ was used on a total of 27 times-of-arrival (TOAs) with the JPL DE200 planetary ephemeris (Standish 1990). The TEMPO package converts each TOA to the solar system barycenter then refines

⁵ <http://pulsar.princeton.edu/tempo>

the timing parameters by minimizing residuals between observed and model TOAs over the observation span. The resulting timing parameters are presented in Table 3. The pulsar’s dispersion measure (DM) of 337 pc cm^{-3} yields an estimated distance of 4.3 kpc using the revised DM-distance model of Cordes & Lazio (2002).

4. DISCUSSION

The position of the 1WGA J1713.4–3949 determined from the *XMM* data is R.A (J2000) $17^{\text{h}} 13^{\text{m}} 28^{\text{s}}.4$, Decl. (J2000) $-39^{\circ}49'54''.5$ (with an uncertainty of $\sim 6''$). Using our 20 cm radio data of SNR G347.3–0.5 obtained with Australia Telescope Compact Array (Lazendic et al. 2003), we found no radio counterpart for 1WGA J1713.4–3949, and derive a 5σ upper limit for a point source flux of 3 mJy. This is similar to the limit derived towards the CCO in Puppis A (Gaensler, Bock, & Stappers 2000). There is no apparent optical emission at the location of 1WGA J1713.4–3949 in the Digitized Sky Survey⁶ image, which has an upper limit of $V > 17 \text{ mag}$.

While the distance to the radio pulsar PSR J1713–3945 is broadly consistent with the SNR distance of $6 \pm 1 \text{ kpc}$ estimated by Slane et al. (1999), the pulsar is likely to be quite old ($\tau_c \sim 1.1 \text{ Myr}$, compared to $\tau < 40 \text{ kyr}$ for SNR G347.3–0.5) and does not have sufficient spin-down luminosity ($\dot{E} \sim 3.7 \times 10^{33} \text{ erg s}^{-1}$) to power the observed X-ray flux from 1WGA J1713.4–3949 ($L_X \sim 6 \times 10^{34} \text{ erg s}^{-1}$). The newly determined radio timing position of the pulsar is $\sim 4'$ in declination away from the position of 1WGA J1713.4–3949 (see Figure 1). PSR J1713–3945 is therefore spatially coincident with SNR G347.3–0.5 by chance, and there is likely no physical association between the two systems. We detected no X-ray source at the position of PSR J1713–3945 in *Chandra* or *XMM* data. Adopting $N_H \sim 5 \times 10^{21} \text{ cm}^{-2}$ (by scaling the value for the SNR to the 4.3 kpc distance of this pulsar), we derive an upper limit on the luminosity in the 0.5–10.0 keV band of $2 \times 10^{31} \text{ erg s}^{-1}$ for nonthermal emission with a photon index ~ 1.5 , and an upper limit on the temperature of 82 eV for blackbody emission from a 10-km radius NS.

The lack of radio and optical counterparts for 1WGA J1713.4–3949, the absence of X-ray pulsations with the current sensitivity and time resolution, the two-component spectrum and its associated luminosity are properties consistent with CCOs (Pavlov et al. 2002).

If this CCO is an accretion powered NS, we can consider two scenarios: accretion from a fallback disk or a low-mass companion. The fallback disk has been suggested to form from residual material after the SNR explosion (e.g., Chevalier 1989) and has been used to explain and unify the properties of various types of NSs (Alpar 2001). However,

limits derived from optical and infrared observations seem to disfavor this model, at least for some types of NSs (e.g., Kaplan et al. 2002). X-ray monitoring, in conjunction with optical and infrared limits, can be used to establish if the NS is variable and thus likely to be accreting from a low-mass companion. Indeed, variability and a period of 6.4 h has been reported for one of the CCOs, J1617–5102 in SNR RCW 103, on which basis this CCO is claimed to be a binary (Sanwal et al. 2002). Comparing the unabsorbed X-ray flux of 1WGA J1713.4–3949 obtained from *Chandra* and *XMM* data for a blackbody fit with that of *ASCA* data ($F_X^0(0.5 - 10.0) = 5.3 \times 10^{-12} \text{ erg cm}^{-2} \text{ s}^{-1}$; Slane et al. 1999), we find no long-term ($\sim 3 \text{ yr}$) variability in 1WGA J1713.4–3949.

Interpretations of the emission from CCOs as thermal radiation from the surface of a NS run into problems due to high surface temperatures and small emitting areas derived from the blackbody model fits. The temperature we derived from the blackbody model of 0.4 keV is much higher than the temperature predicted by the standard cooling model (Page & Sarmiento 1996), while the temperature derived from the NSA models (0.2 keV) would imply an NS age of 100–1000 yr, which is less than the estimated 20–40 kyr age of the SNR (Slane et al. 1999).

In the case that CCOs are rotation powered NSs, the non-detection of radio pulsations can be explained by unfavorable beaming orientation. One of the objects, 1E 1207.4–5209 in SNR G296.5+10.0, that was originally identified as a CCO, has been found to have a period of 424 ms with faint pulsed fraction (7.6%; Zavlin et al. 2000). Our limits on pulsed fraction from 1WGA J1713.4–3949 are consistent with those derived towards other CCOs (7–15%; e.g., Pavlov et al. 2002). Our limits indicate that 1WGA J1713.4–3949 is probably not an AXP, which are generally found to have spin periods between 6–12 s and pulse fractions of 10–70% (e.g., Mereghetti 1998).

In summary, the nature of the compact central object in SNR G347.3–0.5 remains uncertain. Future observations are planned to help determine the exact nature of this source. Pointed *Chandra* observations are needed to provide a more accurate position and to enable a search for an optical counterpart, while deeper timing observations can search for periods substantially shorter than available from the current data.

We thank Peter Woods for useful discussions and Slava Zavlin for providing the files for the magnetic neutron star atmosphere. This work was supported in part by NASA contract NAS8–39073 (POS), grant GO0–1123X (JSL) and grant GO2–3080B (JPH).

REFERENCES

- Alpar, M. A. 2001, *ApJ*, 554, 1245
 Cassam-Chenai, G., Decourchelle, A., Ballet, J., Sauvageot, J.-L., Dubner, G., 2003, *A&A*, in preparation
 Chevalier, R. A. 1989, *ApJ*, 346, 847
 Cordes, J. M. & Lazio, T. J. M. 2002, preprint, astro-ph/0207156
 Crawford, F., Pivovarov, M. J., Kaspi, V. M., & Manchester, R. N. 2002, *ASP Conf. Ser.* 271: Neutron Stars in Supernova Remnants, eds. P. O. Slane & B. M. Gaensler, 37
 Gaensler, B. M., Bock, D. C.-J., & Stappers, B. W. 2000, *ApJ*, 537, L35
 Gänsicke, B. T., Braje, T. M., & Romani, R. W. 2002, *A&A*, 386, 1001
 Gotthelf, E. V., Petre, R., & Vasisht, G. 1999, *ApJ*, 514, L107
 Kaplan, D. L., Kulkarni, S. R., Frail, D. A., & van Kerkwijk, M. H. 2002, *ApJ*, 566, 378
 Lazendic, J., Slane, P., Gaensler, B., Plucinsky, P., Hughes, J. & Reynolds, S., 2003, *ApJ*, submitted

⁶ DSS was produced at the Space Telescope Science Institute under U.S. Government grant NAG W-2166.

- Mereghetti, S. 1998, *Memorie della Societa Astronomica Italiana*, 69, 819
- Pannuti, T., Allen, G., Houck, J., Sturmer, S. 2003, *ApJ*, 593, in press
- Page, D. & Sarmiento, A. 1996, *ApJ*, 473, 1067
- Pavlov, G. G., Shibano, Y. A., Zavlin, V. E., & Meyer, R. D. 1995, in: *The Lives of the Neutron Stars*, eds. M. A. Alpar, U. Kiziloglu, & J. van Paradijs (Kluwer: Dordrecht) p.71.
- Pavlov, G. G., Sanwal, D., Garmire, G. P., & Zavlin, V. E. 2002, *ASP Conf. Ser.* 271: *Neutron Stars in Supernova Remnants*, eds. P. O. Slane & B. M. Gaensler, 247
- Pfeffermann, E. & Aschenbach, B. 1996, *Röntgenstrahlung from the Universe*, eds. Zimmermann, H.U., Trümper, J., and Yorke, H., *MPE Report* 263, 267
- Sanwal, D., Garmire, G. P., Garmire, A., Pavlov, G. G., & Mignani, R. 2002, *American Astronomical Society Meeting*, 200, #72.01
- Standish, E. M. 1990, *A&A*, 233, 252
- Slane, P., Gaensler, B. M., Dame, T. M., Hughes, J. P., Plucinsky, P. P., & Green, A. 1999, *ApJ*, 525, 35
- Thompson, C. 2000, *ASP Conf. Ser.* 202: *IAU Colloq. 177: Pulsar Astronomy - 2000 and Beyond*, 669
- Turner, T. J. & Pounds, K. A. 1986, *MNRAS*, 240, 833
- Vaughan, B. A. et al. 1994, *ApJ*, 435, 362
- Zavlin, V. E., Pavlov, G. G., & Shibano, Y. A. 1996, *A&A*, 315, 141
- Zavlin, V. E., Pavlov, G. G., Sanwal, D., & Trümper, J. 2000, *ApJ*, 540, L25

TABLE 1
PARAMETERS OF THE JOINT SPECTRAL FITS TO THE *Chandra* AND *XMM* SPECTRA OF THE COMPACT SOURCE
1WGA J1713.4–3949 WITH DIFFERENT MODELS.

Model	N_H (10^{21} cm $^{-2}$)	kT (keV)	Γ	R_∞^a (km)	χ^2_{red}/dof	Gain ^b (%)	$F_{X(0.5-10.0)}^{0c}$ (erg cm $^{-2}$ s $^{-1}$)
BREMSS	$7.0^{+0.1}_{-0.2}$	$0.92^{+0.02}_{-0.02}$	—	—	1.07/675	$5.1^{+0.5}_{-0.2}$	9.4×10^{-12}
POW	$10.7^{+0.4}_{-0.2}$	—	$4.2^{+0.1}_{-0.1}$	—	1.44/675	$4.6^{+0.8}_{-0.5}$	3.2×10^{-11}
BB	$3.6^{+0.1}_{-0.1}$	$0.40^{+0.01}_{-0.01}$	—	$2.5^{+0.1}_{-0.1}$	1.25/675	$6.0^{+0.5}_{-0.6}$	4.5×10^{-12}
POW+BB	$8.0^{+0.9}_{-0.6}$	$0.38^{+0.01}_{-0.02}$	$3.9^{+0.3}_{-0.2}$	$2.4^{+0.6}_{-0.4}$	1.05/670	$7.1^{+0.9}_{-0.8}$	$1.4(0.3) \times 10^{-11}$
POW+NSA(G) ^d	$7.3^{+0.6}_{-0.4}$	$0.18^{+0.02}_{-0.01}$	$3.7^{+0.8}_{-0.3}$	$13.0^{+1.0}_{-3.5}$	1.07/670	$5.5^{+0.6}_{-0.5}$	$1.1(0.4) \times 10^{-11}$
POW+NSA(Z) ^e	$8.1^{+1.1}_{-0.9}$	$0.26^{+0.03}_{-0.06}$	$3.8^{+0.2}_{-0.5}$	$15.8^{+4.2}_{-8.4}$	1.22/667	$5.1^{+0.5}_{-0.5}$	$1.5(0.3) \times 10^{-11}$

^aradius of the emitting region at infinity assuming the source distance of 6 kpc

^ba linear gain shift included for fitting the *Chandra* data

^cunabsorbed flux — for the two component models the flux of the second component alone is given in parentheses

^dNSA model by Gänsicke, Braje, & Romani (2002) for weak magnetic field of $\leq 10^{10}$ G

^eNSA model by Pavlov et al. (1995) for standard magnetic field of 10^{12} G

TABLE 2
PARAMETERS AND RESULTS OF PULSATION SEARCH FROM 1WGA J1713.4–3949 USING FFT.

Detector	Time resolution	Frequency range searched	f_p limit ^a
ACIS-S1	3.2 s	0.01–0.16 Hz	12%
EPIC-MOS ^b	2.6 s	0.01–0.19 Hz	12%
EPIC-pn	199 ms	0.01–2.5 Hz	4%
PCA ^c	4 ms	0.01–128 Hz	25%

^afractional pulsation upper limit to 99% confidence level
calculated according to Vaughan et al. (1994)

^bfrom combined MOS1 and MOS2 data

^ccalculated from FFT of two separate intervals of ~ 3
days of data with gaps

TABLE 3
PROPERTIES OF THE RADIO PULSAR PSR J1713–3945 DETECTED TOWARDS G347.3–0.5.

Parameter	Value ^a
R.A. (J2000)	17 ^h 13 ^m 14 ^s 23(3)
Decl. (J2000)	−39°45′47″5(14)
Period, P (ms)	392.451769234(8)
Period derivative, \dot{P} ($\times 10^{-15}$)	5.7380(5)
Dispersion Measure, DM (pc cm ^{−3})	337(3)
Epoch of period (MJD)	52165.0
rms residual (ms)	1.1
Number of TOAs	27
Timing span (Days)	1200
Characteristic age, ^b τ_c (Myr)	1.08
Surface magnetic field, ^c B ($\times 10^{12}$ G)	1.52
Spin-down luminosity, ^d \dot{E} (erg s ^{−1})	3.74×10^{33}

^aValues in parentheses represent the 1σ uncertainty in the least significant digit quoted.

$$^b\tau_c \equiv P/2\dot{P}$$

$$^cB \equiv 3.2 \times 10^{19} (P\dot{P})^{1/2} \text{ G, where } P \text{ is in seconds}$$

$$^d\dot{E} \equiv 4\pi^2 I \dot{P} / P^3, \text{ with } I = 10^{45} \text{ g cm}^2 \text{ assumed}$$

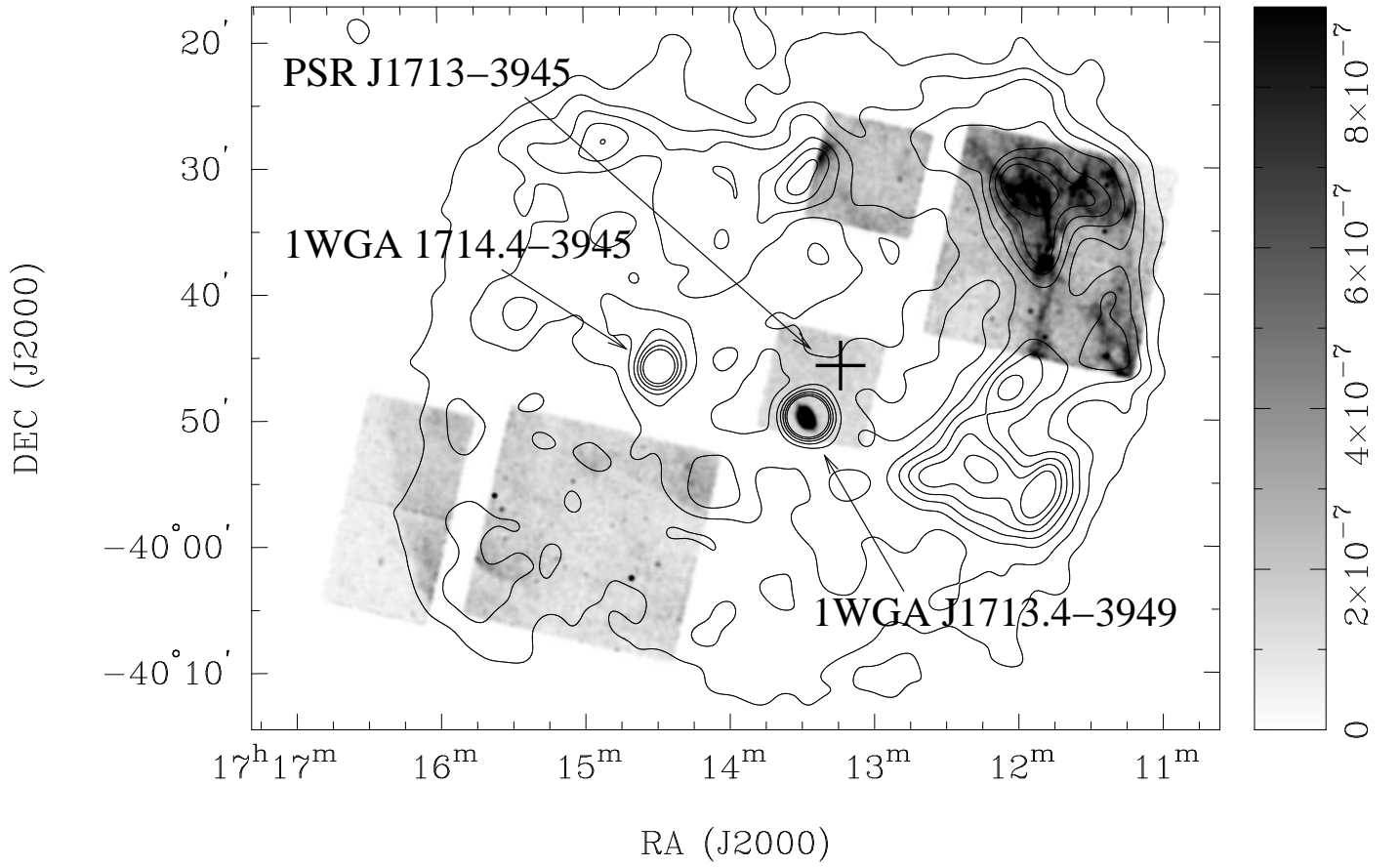


FIG. 1.— The 0.5-10.0 keV band *Chandra* grayscale image of the two fields observed towards the SNR G347.3-0.5 (for more details see Lazendic et al. 2003). To show the whole extent of the remnant, the *Chandra* image is overlaid with the *ROSAT* PSPC contours (Slane et al. 1999). Two point sources detected with *ROSAT* observations are labeled, as well as the location of the radio pulsar PSR J1713-3945.

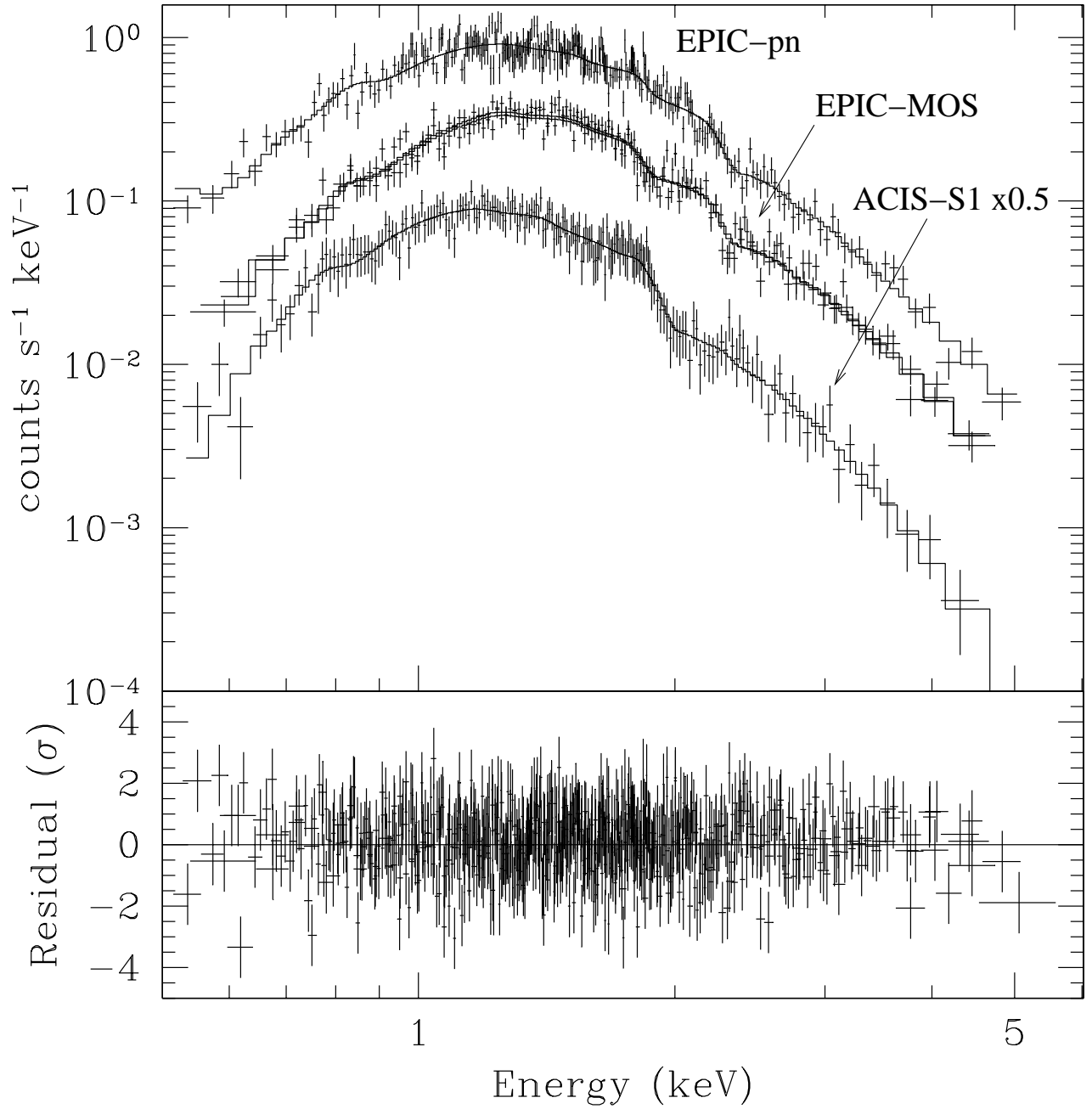


FIG. 2.— ACIS and EPIC spectra from the compact source 1WGA J1713.4–3949 and residuals for blackbody+power law model. The fit parameters are listed in Table 1.